Environmental and Climate Technologies
2024, vol. 28, no. 1, pp. 464–476
https://doi.org/10.2478/rtuect-2024-0036
https://content.sciendo.com

Optimizing External-Heating Gasifiers for Enhanced Efficiency: A Synergistic Approach with Taguchi's Method in Support of Climate Change Mitigation Goals

Chung-Neng HUANG[1*], Yu-Chang YEN[2]

[1,2]*National University of Tainan, 33, Sec. 2, Shu-Lin St. Tainan, Taiwan*

Received 21.03.2024; accepted 25.09.2024

***Abstract* – To limit global warming to 1.5 °C and adhere to the Paris Agreement's targets, urgent action is imperative. The IPCC stresses a 45 % CO_2 reduction by 2030 or a 25 % reduction to cap temperature rise at 2 °C, with failure risking greater challenges and costs. Enhancing energy efficiency, particularly through hydrogen utilization, is crucial. Gasifiers offer promise but face efficiency issues, addressed here with external-heating gasifiers leveraging waste heat. This nonlinear problem is optimized using Taguchi's method, facilitated by COMSOL Multiphysics software. The study contributes to environmental sustainability and carbon reduction efforts, emphasizing the potential of external-heating gasifiers for a sustainable energy future.**

***Keywords* – External Heating Gasifier; hydrogen; optimal design; Taguchi's method.**

1. INTRODUCTION

The urgent imperative to limit the global average temperature increase to 1.5 °C, as outlined in the Paris Agreement [1], demands comprehensive efforts for effective climate change mitigation [2]. The Intergovernmental Panel on Climate Change (IPCC) stresses the need to reduce carbon dioxide emissions by 45 % by 2030 or achieve a 25 % reduction to cap the temperature rise at 2 °C [2]. Failure to meet these targets by 2030 could pose significant challenges in achieving net-zero emissions, potentially incurring higher costs [2]. This research aligns with the global commitment to climate change mitigation, contributing to the broader context of environmental sustainability and carbon reduction.

Recognizing energy efficiency as a key strategy in addressing climate change challenges [3], hydrogen emerges as a promising solution, known for its high efficiency and zero emissions during combustion [4]–[5]. However, traditional gasifiers, commonly used to transform affordable fuels like coal or biomass into hydrogen, face inherent energy-intensive characteristics [6]. In response, the concept of an external-heating gasifier is introduced, utilizing waste heat generated by boilers or fuel cells.

The design of an external-heating gasifier presents a classic nonlinear challenge. Achieving optimal performance requires an innovative approach, with the integration of Taguchi's method proving significant. This paper leverages advanced methodologies to optimize

* Corresponding author.
E-mail address: kosono@mail.nutn.edu.tw

external-heating gasifiers, contributing to the evolution of cleaner and more efficient energy production methods.

To provide a comprehensive understanding of the current state of the field, this research draws insights from various studies related to hydrogen production [4]–[7], direct hydrocarbon fuel cells [7], biofuel production [8], and hydrogen production in nuclear cogeneration cycles [9]. Additionally, literature on gasification processes [10]–[14], heat exchanger optimization [15]–[17], and advanced optimization techniques such as neural-network-based machine learning [18]–[20] serves as a foundation for the proposed methodology.

This study, focusing on the integration of Taguchi's method, strives to address the challenges associated with gasifier optimization. The presented methodology not only contributes to the ongoing discourse on sustainable energy but also aims to propel advancements in the field of hydrogen production and gasification processes [21]. The effectiveness of the proposed approach is validated through a simulation study on an existing gasifier, highlighting its potential for real-world applications in the pursuit of a sustainable energy future.

2. DESCRIPTION OF CASE STUDY

Plasma coal gasification uses plasma torches – devices that generate extremely high temperatures (up to 5000–7000 °C) – to convert coal into syngas (synthetic gas) in an oxygen-starved environment. This process, unlike traditional coal combustion, does not burn coal directly, but instead breaks it down into simpler chemical components. The key outputs from plasma gasification include:

Syngas: A mixture primarily of hydrogen (H_2) and carbon monoxide (CO), which can be further processed or used as a cleaner energy source.

Slag: An inert, glass-like material formed from the inorganic components of coal, which can be used in construction or disposed of without environmental hazards.

Plasma gasification of coal reduces CO_2 emissions by converting coal into syngas, which can be used more efficiently than direct coal combustion in combined cycle power plants. These plants utilize both gas and steam turbines, increasing efficiency and reducing CO_2 output per unit of energy. Additionally, hydrogen can be separated from syngas and used as a zero-emission fuel. Plasma gasification also avoids the large-scale production of CO_2 and other pollutants typical of coal combustion by controlling oxygen levels, producing primarily carbon monoxide, which can be captured or converted. The process is highly compatible with carbon capture technologies, as it creates a concentrated CO_2 stream, making storage easier and more efficient [22].

In this paper, the Plasma Coal Gasification System (Plasma CGS) used by Serbin *et al.* [23] is adopted as the model for gasification. The Plasma CGS operates at a high temperature (above 1273 K), closely resembling the operational temperature of Solid Oxide Fuel Cells (SOFC) (approximately 1250 K [24]). Given the compatibility of SOFC with waste heat recovery, the integration of a gasifier with a fuel cell can enhance gasifier efficiency. The gasifier, in turn, provides the necessary fuel for the fuel cell, creating a symbiotic relationship. This paper utilizes the Plasma CGS as the gasifier model, as illustrated in Fig. 1. Given the challenges and costs associated with modifying existing institutional designs, this study proposes an External-Heating Gasifier that efficiently recovers external waste heat without altering the gasifier's internal design. The study utilizes Taguchi optimization to address uneven temperature distribution issues effectively.

While the use of plasma air for gasifier heating results in high temperatures (approximately 4000 K), it shortens the system's lifespan (approximately 300–500 hours). Lowering the mass flow rate (approximately 2 g/s) is required to reach the temperature needed for coal gasification. However, this can lead to uneven temperature distribution within the gasifier. Though most temperatures are above the minimum working temperature (approximately 1273 K), the lower temperatures may reduce gasification efficiency, while higher temperatures result in energy wastage.

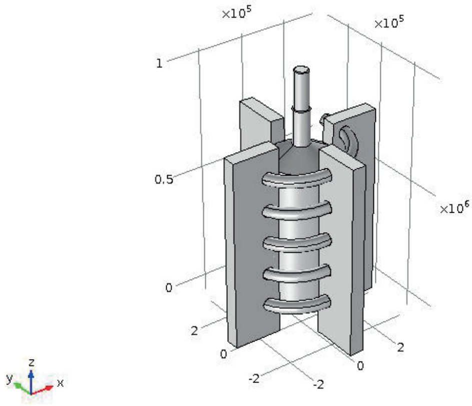

Fig. 1. External Heating Gasifier.

For ease of identifying parameters leading to fast heating and uniform temperature distribution, measurement points at the top, middle, and bottom layers of the gasifier's center are chosen (labelled as P1, P2, and P3 in Fig. 2). Simulations are conducted to calculate the time required for these points to reach a stable temperature. Stability is defined within 5 % of the final set temperature (1187 K) commonly used in control theory. The heating speed is determined by the time required for the latest point to reach stability, while uniformity is measured by the average time difference among the three measurement points.

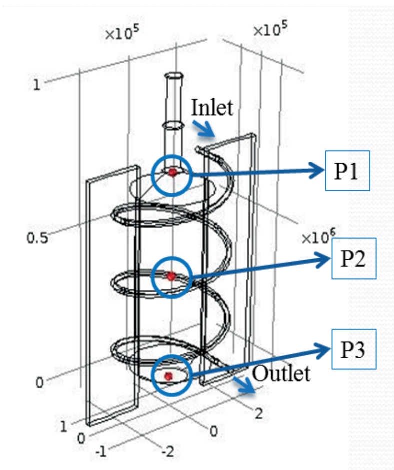

Fig. 2. Measurement points.

2.1. Design and Analysis of External-Heating Gasifier

COMSOL is employed for thermal analysis, with copper selected as the solid heat-conducting material. The contact surfaces between the heat pipe and fins, as well as the fins and gasifier, are treated as thermal walls, while other contact surfaces are treated as insulating walls. The working fluid is assumed to be water vapour, with an inlet temperature of 1250 K [24], a mass flow rate of 51 g/s [25], and a gasifier's minimum working temperature of 755 K [23].

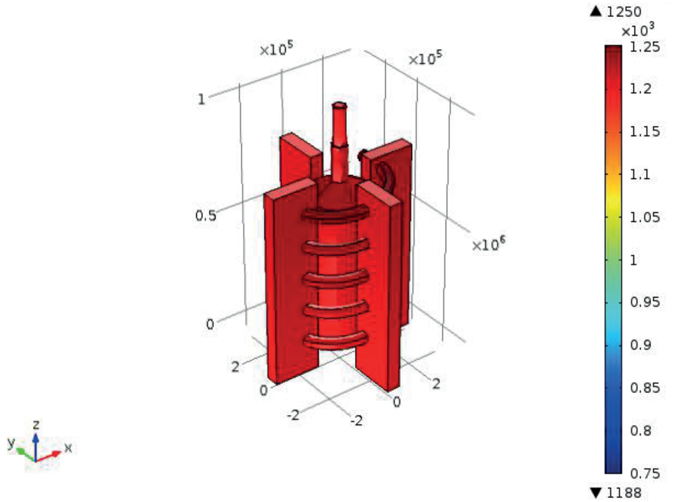

Fig. 3. Prototype heat distribution map.

The results from the COMSOL simulations for the prototype indicate that the stabilization times for P1, P2, and P3 are 80, 84, and 90 minutes, respectively, as presented in Table 1. Fig. 3 depicts the heat distribution at the 90-minute mark.

TABLE 1. STABILIZATION TIMES FOR PROTOTYPE MEASUREMENT POINTS

P1	P2	P3	Stabilization time	Heat distribution uniformity
80	84	90	90	(4+6+10)/3 = 6.6

These findings provide valuable insights into the feasibility and performance of the proposed External-Heating Gasifier, showcasing its potential for efficient waste heat recovery and uniform temperature distribution. The integration of external waste heat not only avoids the complexities and costs associated with modifying internal designs but also enhances the gasifier's overall efficiency.

3. OPTIMAL DESIGN

The Taguchi method, pioneered by Dr Genichi Taguchi in the field of quality engineering, has been instrumental in swiftly addressing engineering problems. Although considerable time has passed since its inception, the Taguchi method remains essential for resolving current engineering challenges. In recent years, numerous studies have successfully applied the Taguchi method to various domains. Chen *et al.* [26] optimized a fluidized bed gasifier for hydrogen production from biomass (eucalyptus) using the Taguchi method, achieving a charcoal conversion efficiency of 94.51 %. Alzoubi *et al.* [27] proposed using the Taguchi method to optimize a finned-tube heat exchanger for improved performance and efficiency. Etghani *et al.* [28] applied the Taguchi method to enhance a shell-and-tube spiral heat exchanger, identifying optimal heat transfer parameters. These studies demonstrate the feasibility of applying the Taguchi method for optimization in recent years, both in gasifiers and heat exchangers.

3.1. Controllable Factors

To achieve optimal system design, identifying control factors within the system is crucial. This system primarily involves the combination of fins and heat pipes. Therefore, the controllable variables are the fin and heat pipe components. For the heat pipe, controllable factors include diameter, winding method, and the number of turns. Since the heat pipe's impact on heat exchange determines the important factor of waste heat from the fuel cell entering the gasifier, and all three factors are within controllable ranges, this study includes all three components of the heat pipe as control factors for subsequent analysis. Regarding fins, controllable factors include length, quantity, height, and thickness. The length represents the distance between the gasifier and the heat pipe, constrained by the pipe diameter and the distance between the heat pipe and the gasifier. As the extended portion beyond the heat pipe has a minor impact on heat exchange, with the main heat exchange occurring in the space between the heat pipe and the gasifier, the fin length is set as a fixed value. The number of fins represents the contact area between the fins and the heat pipe, as well as the fins and the gasifier, making it a crucial factor for heat exchange. The fin height uses the gasifier's intrinsic height without affecting heat exchange. The fin thickness determines the critical effective contact area in the heat exchange system. Thus, this study includes fin thickness as a control factor.

In summary, the identified control factors from heat pipes and fins are the winding method, fin quantity, fin thickness, heat pipe turns, and pipe diameter. To facilitate Taguchi method calculations, each of these five control factors is further investigated for control parameters. These control factors are discussed and set as follows:

Winding Method: Two winding methods, spiral and multiple-loop designs, are considered for even heating, as shown in Fig. 4.

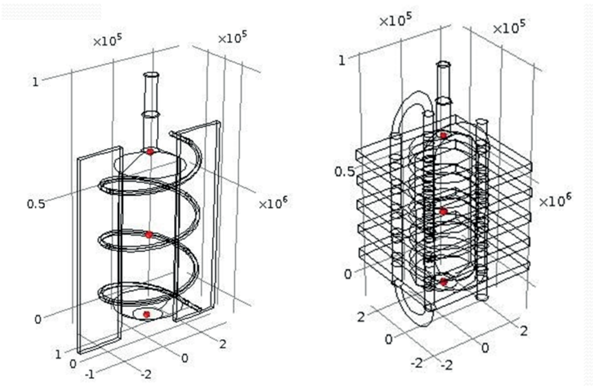

(a) Spiral design (b) Multiple loop design

Fig. 4. Winding methods.

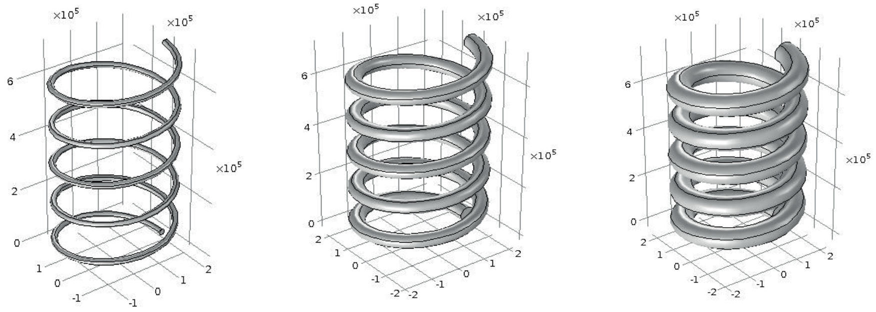

(a) 10 mm (b) 25 mm (c) 40 mm

Fig. 5. Pipe diameter.

Pipe Diameter: Using the common specifications of current copper pipes as the standard design, the maximum and minimum pipe diameters are considered as parameter limits. The average of these limits is taken as the original parameter, with values of 10 mm, 25 mm, and 40 mm (as shown in Fig. 5).

Turns of Heat Pipe: To meet spatial constraints and effectiveness, the minimum turn design is set at three turns. As the number of turns must ensure that all parameters are valid and do not interfere with each other, the maximum parameter affecting the turns is the pipe diameter. This study deploys the largest pipe diameter in the experimental space, determining the maximum turns as seven turns. The average of these maximum and minimum turn values is taken as the original parameter, with values of 3 turns, 5 turns, and 7 turns (as shown in Fig. 6).

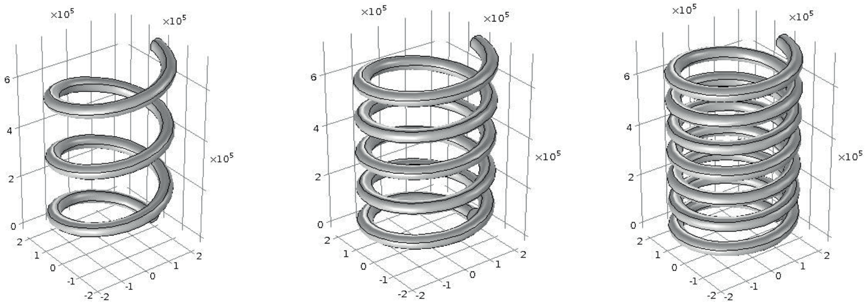

(a) 3 turns (b) 5 turns (c) 7 turns

Fig. 6. Turns of heat pipe.

Fin Thickness: Limitations mainly arise in the design with multiple loops. Considering the effective space within the gasifier and the maximum allowable fin thickness, the maximum fin thickness is 60 mm without interference. The minimum thickness must maintain the basic contact area with the gasifier, thus set at 20 mm. The original parameter is set as the average of these maximum and minimum values, i.e., 40 mm.

Fin Quantity: Due to spatial design considerations, under the maximum fin thickness condition, the maximum allowable quantity is six in the case of a spiral design to prevent fin interference. To ensure uniform heating, a minimum of two fins is needed to provide the fins with their intrinsic meaning. For effective use of the Taguchi method in finding optimal parameters, a set of middle values is chosen as the original parameters, with control parameters of 2 fins, 4 fins, and 6 fins.

Combining the above analyses, the control factors are recorded in Table 2. Due to only two control factors in category A, Level 1 is set as the original parameter. This encompasses pipe diameter, turns of pipe, fin thickness, and fin quantity, all of which are vital factors in the heat exchange process for the Taguchi method's optimal design.

TABLE 2. CONTROL FACTOR LEVEL TABLE

Control Factors	Descriptions	Level 1	Level 2	Level 3
A	Winding method	Spiral	Multiple-Loop	
B	Pipe diameter	10	25	40
C	Turns of pipe	3	5	7
D	Fin thickness	20	40	60
E	Fin quantity	2	4	6

4. RESULTS AND DISCUSSIONS

In order to determine the time required for each measurement point to reach a stable temperature, the COMSOL simulation software is employed to identify the time at which P1, P2, and P3 reach stable temperatures. Given that the research objective is to find the parameter design that achieves the fastest stabilization time, where smaller times are preferred, the Signal-to-Noise (S/N) ratio is calculated using the Taguchi method's Signal-to-Noise ratio formula Eq. (1). An L18 orthogonal array, the time for each point to reach a stable temperature, and the average and *S*/*N* are presented in Table 3.

$$\frac{S}{N} = -10\log\left[\frac{\sum_{i=1}^{n} y_i^2}{n}\right] = -10\log\left[\,\overline{y}^2 + S_n^2\,\right] \quad (1)$$

When a factor changes from one level to another, both the *S*/*N* value and the quality characteristics will vary, known as Factor Effects. After calculating the *S*/*N* ratio values for each factor at different levels, the results were presented in Table 4. The factor effects, E^{1-2}, represent the change in the SN ratio when the factor shifts from the first to the second level, while E^{2-3} represents the change when the factor shifts from the second to the third level. These values were determined for each parameter and included in the table. A larger range value (E^{2-3}–E^{1-2}) indicates a greater influence of the variable on the process.

TABLE 3. L_{18} ORTHOGONAL ARRAY AND SIMULATION DATA

Exp.	A	B	C	D	E	P1	P2	P3	Mean	S	S/N
1	1	1	1	1	1	160	164	162	162.000	2.00000	–44.1907
2	1	1	2	2	2	88	90	90	89.333	1.15470	–39.0208
3	1	1	3	3	3	78	80	82	80.000	2.00000	–38.0636
4	1	2	1	1	2	86	88	88	87.333	1.15470	–38.8241
5	1	2	2	2	3	84	88	92	88.000	4.00000	–38.8956

6	1	2	3	3	1	56	54	54	54.667	1.15470	–34.7557
7	1	3	1	2	1	52	52	52	52.000	0.00000	–34.3201
8	1	3	2	3	2	72	78	82	77.333	5.03322	–37.7796
9	1	3	3	1	3	54	56	60	56.667	3.05505	–35.0750
10	2	1	1	3	3	100	96	98	98.000	2.00000	–39.8257
11	2	1	2	1	1	90	100	90	93.333	5.77350	–39.4118
12	2	1	3	2	2	110	106	108	108.000	2.00000	–40.6695
13	2	2	1	2	3	90	88	90	89.333	1.15470	–39.0208
14	2	2	2	3	1	66	76	68	70.000	5.29150	–36.9185
15	2	2	3	1	2	132	132	134	132.667	1.15470	–42.4555
16	2	3	1	3	2	74	74	74	74.000	0.00000	–37.3846
17	2	3	2	1	3	72	70	70	70.667	1.15470	–36.9851
18	2	3	3	2	1	54	54	60	56.000	3.46410	–34.9748

TABLE 4. L_{18} S/N RESPONSE TABLE

Level	**A**	**B**	**C**	**D**	**E**
1	–37.88	–37.43	–39.49	–38.93	–40.20
2	–38.63	–39.36	–37.82	–38.17	–38.48
3		–37.98	–37.45	–37.67	–36.09
$E^{1–2}$	–0.75	–1.93	1.67	0.76	1.72
$E^{2–3}$		1.38	0.37	0.5	2.39
Range	0.75	1.93	2.04	1.26	4.11
Rank	5	3	2	4	1
Significant?	No	Yes	Yes	No	Yes

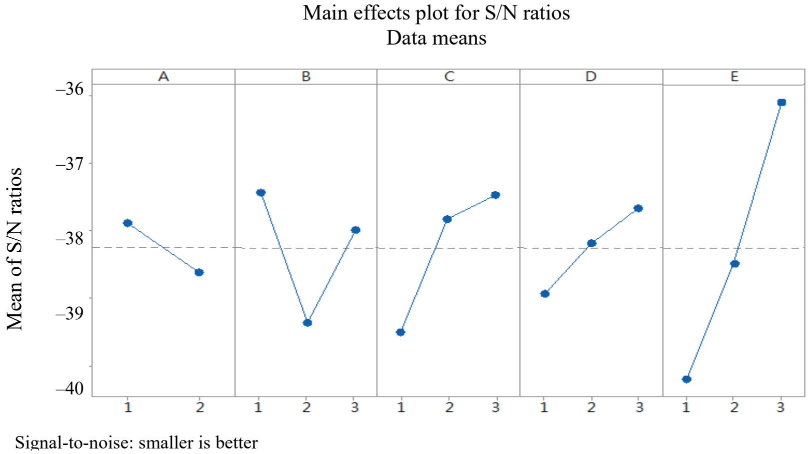

Fig. 7. S/N response chart.

The factors are ranked based on the Range, with the top three factors chosen for experimentation based on the One-Half Criterion. The selected key factors are *B* (pipe diameter), *C* (turns of pipe), and *E* (fin quantity). The numerical values from Table 4 are plotted in the *S*/*N* response chart in Fig. 7.

A larger amplitude in the *S*/*N* response chart indicates a greater influence and importance of the control factor on product design outcomes. A higher *S*/*N* value represents a more stable quality. From Fig. 7, the level with the maximum *S*/*N* for each control factor is chosen as the optimal control factor, resulting in the best combination of A1B1C3D3E3. This represents the spiral heat pipe arrangement with 6 fins, fin thickness of 60 mm, 7 winding turns, and a diameter of 10 mm. This is considered the optimal parameter combination for *S*/*N*.

In the optimization design, although *S*/*N* is effective in reducing the variability of quality characteristics, relying solely on *S*/*N* ratios as the basis for optimization results is insufficient. Therefore, an analysis of quality characteristics is imperative. As recorded in Table 2, the average values of each level for all factors are documented in the Quality Characteristic Response Table (Table 5). Subsequently, based on the calculated influences of each level, *E* (Fin Quantity) emerges as the primary control factor, followed by *C* (Heat Pipe Coiling Turns) as the secondary control factor. The Quality Characteristic Response Chart, depicted in Fig. 8, is generated based on the average values of each level in Table 4.

TABLE 5. QUALITY CHARACTERISTIC RESPONSE TABLE

Level	A	B	C	D	E
1	83.04	81.33	100.44	93.78	105.11
2	88.00	94.78	80.44	81.44	87.00
3		80.44	75.67	81.33	64.44
E^{1-2}	4.96	13.45	–20	–12.34	–18.11
E^{2-3}		–14.34	–4.77	–0.11	–22.56
Range	4.96	14.34	24.77	12.45	40.67
Rank	5	3	2	4	1
Significant?	No	Yes	Yes	No	Yes

units: minutes

Due to the fact that the calculated quality characteristic is the minimization of the required heating time, the optimal result is chosen by selecting the minimum value of the quality characteristic among the levels in Fig. 8.

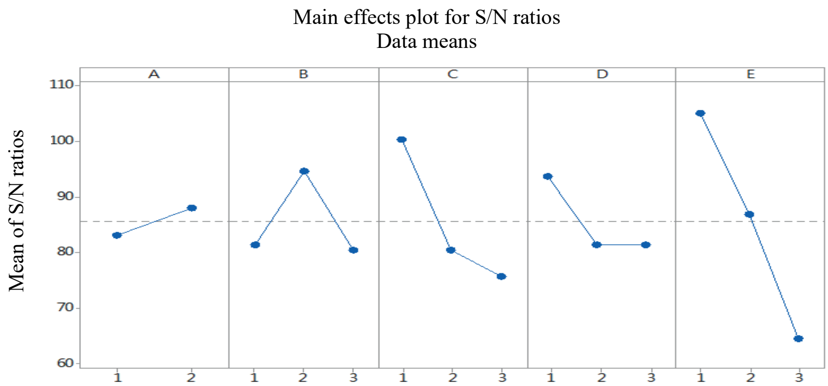

Fig. 8. Quality characteristic response chart.

The optimal result affecting the quality characteristic is A1B3C3D3E3. After comparing the results of the *S*/*N* response (Table 4) and the quality characteristic response (Table 5), it can be observed that the ranking of factors influencing the quality is consistent, and among the critical factors, the optimization results are the same for all factors except factor B (heat pipe diameter). Therefore, as a compromise, the optimal result should be A1B2C3D3E3.

TABLE 6. COMPARISON OF OPTIMIZATION RESULTS WITH ORIGINAL AND OPTIMAL DESIGNS

	A	B	C	D	E	P1	P2	P3	Time, min,
Original	1	2	2	2	2	80	84	90	90
Optimal	1	2	3	3	3	28	30	34	34

Table 6 shows that, based on the optimal design, the time required for all measurement points to reach a stable temperature is 34 minutes. Compared to the original design's 90 minutes to reach stability, the heating time has been reduced by 62 %. To facilitate a comparison of the thermal distribution diagrams between the original and optimal designs at 34 minutes, they are represented in Fig. 9, it can be observed that the temperature of the optimal design is significantly higher than that of the original design. According to Table 7, the temperature at each measurement point has increased by a minimum of 160.9 K, with the average temperature rising by 177.8 K. The temperatures of each measurement point at 34 minutes are recorded in Table 7.

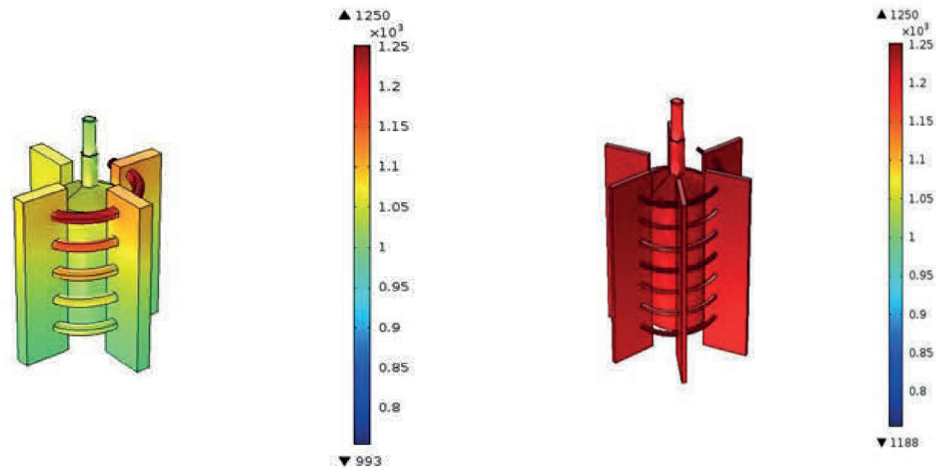

Fig. 9. Thermal distribution diagram at 34 minutes.

TABLE 7. TEMPERATURE AT EACH MEASUREMENT POINT AT 34 MINUTES

	P1	P2	P3	Ave.	Minimum
Original	1052.8	1028.3	1000.5	1027.2	1052.8
Optimal	1213.7	1206.4	1195.0	1205.0	1213.7
Increasement	160.9	178.0	194.6	177.8	160.9

units: K

5. CONCLUSION

This paper presents several innovations and contributions:

Introduction of External-Heating Gasifiers: The paper introduces the concept of external-heating gasifiers, which utilize waste heat generated by boilers or fuel cells to improve efficiency. This approach offers a novel solution to address the energy-intensive characteristics of traditional gasifiers.

Integration of Taguchi's Method: The study implements Taguchi's method, a robust optimization technique, to achieve optimal performance of external-heating gasifiers. This synergistic approach demonstrates the effectiveness of combining advanced methodologies for system optimization.

Simulation Platform Development: The research develops a simulation platform using COMSOL Multiphysics software to facilitate the integration of Taguchi's method. This platform enables comprehensive analysis and optimization of external-heating gasifiers.

Reduction of Heating Time: Through optimization using Taguchi's method, the paper demonstrates a significant reduction in heating time for gasifiers, thereby enhancing efficiency and reducing energy consumption.

Contribution to Climate Change Mitigation: By improving the efficiency of gasification processes, the paper contributes to broader goals of climate change mitigation. The findings underscore the potential of external-heating gasifiers in reducing carbon emissions and promoting sustainable energy practices.

Environmental Impact Analysis: The platform could be used to model the environmental impacts of the gasification process, such as emissions of greenhouse gases, particulates, or toxic by-products. Researchers can simulate different scenarios to minimize the environmental footprint, aiding in the development of more sustainable gasification technologies.

Testing Alternative Feedstocks: Future research could leverage the simulation platform to explore the use of alternative feedstocks, such as biomass, municipal waste, or industrial residues, in the External-Heating Gasifier. This would allow for investigating the potential of using renewable or waste materials in the gasification process, thereby reducing reliance on fossil fuels and lowering the overall carbon footprint.

Integration with Carbon Capture Technologies: The simulation tool can be used to model and test the integration of carbon capture and storage (CCS) technologies within the gasification process. This would help researchers understand how to efficiently capture CO_2 produced during gasification and explore strategies to retrofit existing systems or design new gasifiers with built-in CCS capabilities.

Exploring Hybrid Systems: The simulation platform can be applied to research on hybrid energy systems that combine external-heating gasifiers with renewable energy sources, such as solar or wind. By simulating the interactions between gasification and renewable power sources, researchers can design hybrid systems that reduce reliance on fossil fuels while maintaining energy reliability and output.

Overall, the paper provides valuable insights and methodologies for optimizing gasification systems, advancing the transition towards cleaner and more efficient energy production methods in alignment with climate change mitigation objectives.

ACKNOWLEDGEMENT

This work has been supported by the National Science and Technology Council, TAIWAN within the project "Development of a Novel Wireless and Distribution Charging System for the 3D Mechanical Garages" No. 111-2221-E-024 -005 -MY3.

REFERENCES

[1] Full report – Statistical Review of World Energy 2021 – B. [Online]. [Accessed 15.04.2024]. Available: https://www.bp.com/

[2] A New Report from IPCC – Climate Change Science. [Online]. [Accessed 15.04.2024]. Available: https://talkofthecities.iclei.org/

[3] Energy – accelerating the transition from coal to clean power. [Online]. [Accessed 15.04.2024]. Available: https://ukcop26.org/energy/

[4] Hisatomi T., Domen K. Reaction systems for solar hydrogen production via water splitting with particulate semiconductor photocatalysts. *Nature Catalysis* 2019:2:387–399. https://doi.org/10.1038/s41929-019-0242-6

[5] Rieksta M., Zarins E., Bazbauers G. Potential Role of Green Hydrogen in Decarbonization of District Heating Systems: A Review. *Environmental and Climate Technologies* 2023:27(1):545–558. https://doi.org/10.2478/rtuect-2023-0040

[6] Akhlaghi N., Najafpour-Darzi G. A comprehensive review on biological hydrogen production. *International Journal of Hydrogen Energy* 2020:45(43):22492–22512. https://doi.org/10.1016/j.ijhydene.2020.06.182

[7] Mohammed H., Al-Othman A., Nancarrow P., Tawalbeh M., Assad M. E.-H. Direct hydrocarbon fuel cells: A promising technology for improving energy efficiency. *Energy* 2019:172:207–219. https://doi.org/10.1016/j.energy.2019.01.105

[8] Satari B., Karimi K., Kumar R. Cellulose solvent-based pretreatment for enhanced second-generation biofuel production: a review. *Sustainable energy & fuels* 2019:11–62. https://doi.org/10.1039/C8SE00287H

[9] Kowalczyk T., Badur J., Bryk M. Energy and exergy analysis of hydrogen production combined with electric energy generation in a nuclear cogeneration cycle. *Energy Conversion and Management* 2019:198:111805. https://doi.org/10.1016/j.enconman.2019.111805

[10] Arabloo M., BahadoriA., Ghiasi M. M., Lee M., Zendehboudi A. A. S. A novel modeling approach to optimize oxygen-steam ratios in coal gasification process. *Fuel* 2015:153:1–5. https://doi.org/10.1016/j.fuel.2015.02.083

[11] Mularski J., Pawlak-Kruczek H., Modlinski N. A review of recent studies of the CFD modelling of coal gasification in entrained flow gasifiers, covering devolatilization, gas-phase reactions, surface reactions, models and kinetics. *Fuel* 2020:271:117620. https://doi.org/10.1016/j.fuel.2020.117620

[12] Pandey D. S., Pan I., Das S., Leahy J. J., Kwapinski W. Multi-gene genetic programming based predictive models for municipal solid waste gasification in a fluidized bed gasifier. *Bioresource Technology* 2015:179:524–533. https://doi.org/10.1016/j.biortech.2014.12.048

[13] Sadasivam S., Zagorščak R., Thomas H. R., Kapusta K. Experimental study of methane-oriented gasification of semi-anthracite and bituminous coals using oxygen and steam in the context of underground coal gasification (UCG): Effects of pressure, temperature, gasification reactant supply rates and coal rank. *Fuel* 2020:268:117330. https://doi.org/10.1016/j.fuel.2020.117330

[14] Kutnyi B., Pavlenko A., Cherednikova O. Theoretical Foundations of Gas Hydrate Synthesis Intensification. *Environmental and Climate Technologies* 2023:27(1):666–682. https://doi.org/10.2478/rtuect-2023-0049

[15] Etghani M. M., Baboli S. A. H. Numerical investigation and optimization of heat transfer and exergy loss in shell and helical tube heat exchanger. *Applied Thermal Engineering* 2017:121:294–301. https://doi.org/10.1016/j.applthermaleng.2017.04.074

[16] Li C., Guan Y., Feng Y., Jiang C., Zhen S., Su X. Comparison of influencing factors and level optimization for heating through deep-buried pipe based on Taguchi method. *Geothermics* 2021:91:102045. https://doi.org/10.1016/j.geothermics.2021.102045

[17] Pandey N., Murugesan K., Thomas H. R. Optimization of ground heat exchangers for space heating and cooling applications using Taguchi method and utility concept. *Applied Energy* 2017:190:421–438. https://doi.org/10.1016/j.apenergy.2016.12.154

[18] Qi X., Chen G., Li Y., Cheng X., Li C. Applying Neural-Network-Based Machine Learning to Additive Manufacturing: Current Applications, Challenges, and Future Perspectives. *Engineering* 2019:5(4):721–729. https://doi.org/10.1016/j.eng.2019.04.012

[19] Zhang Z., Liu S., Gao W., Xu J., Zhu S. An enhanced multi-objective evolutionary optimization algorithm with inverse model. *Information Sciences* 2020:530:128–147. https://doi.org/10.1016/j.ins.2020.03.111

[20] Jin J., Feng F., Na W., Yan S., Liu W., Zhu L., Zhang Q., Recent advances in neural network-based inverse modeling techniques for microwave applications. *International Journal of Numerical Modeling: Electronic Networks, Devices and Fields* 2020:33(6):e2732. https://doi.org/10.1002/jnm.2732

[21] Luca A., Ragazzi M., Tubino M., Schiavon M. Criteria for Enhanced Monitoring and Control Plans for a Waste Gasification Plant. *Environmental and Climate Technologies* 2023:27(1):570–580. https://doi.org/10.2478/rtuect-2023-0042

[22] Zhuk H., Ivanov Y., Onopa L., Krushnevych S., Soltanibereshne M. Effectiveness of Water-Amine Combined Process for CO_2 Extraction from Biogas. *Environmental and Climate Technologies* 2024:28(1):135–148. https://doi.org/10.2478/rtuect-2024-0012

[23] Serbin S. I., Matveev I. B. Theoretical Investigations of the Working Processes in a Plasma Coal Gasification System. *IEEE Transactions on Plasma Science* 2010:38(12):3300–3305. https://doi.org/10.1109/TPS.2010.2086495

[24] Laoun B., Belhamel M. A Three Dimensional Model to Simulate Power Performance of a Single Solid Oxide Fuel Cell. *2nd International Symposium on Environment-Friendly Energies and Applications* (EFEA). June, 2012. https://doi.org/10.1109/EFEA.2012.6294070

[25] Lakshmi T. V. V. S., Geethanjali P., Krishna P. S. Mathematical modelling of solid oxide fuel cell using Matlab/Simulink. *International Conference on Microelectronics, Communication and Renewable Energy* (ICMiCR-2013). 2013. https://doi.org/10.1109/AICERA-ICMiCR.2013.6576016

[26] Chen W. H., Chen C. J., Hung C. I. Taguchi approach for co-gasification optimization of torrefied biomass and coal, *Bioresource Technology* 2013:144:615–622. https://doi.org/10.1016/j.biortech.2013.07.016

[27] Alzoubi M. A., Sasmito A. P. Thermal performance optimization of a bayonet tube heat exchanger. *Applied Thermal Engineering* 2017:111:232–247. https://doi.org/10.1016/j.applthermaleng.2016.09.052

[28] Etghani M. M., Baboli S. A. H. Numerical investigation and optimization of heat transfer and exergy loss in shell and helical tube heat exchanger. *Applied Thermal Engineering* 2017:121:294–301. https://doi.org/10.1016/j.applthermaleng.2017.04.074